

Published in final edited form as:

Circ Res. 2012 June 8; 110(12): 1564–1574. doi:10.1161/CIRCRESAHA.112.269795.

***NPHP4* Variants are Associated with Pleiotropic Heart Malformations**

Vanessa M. French^{1,15}, Ingrid M.B.H. van de Laar^{1,15}, Marja W. Wessels¹, Christan Rohe¹, Jolien W. Roos-Hesselink², Guangliang Wang³, Ingrid M.E. Frohn-Mulder⁴, Lies-Anne Severijnen¹, Bianca M. de Graaf¹, Rachel Schot¹, Guido Breedveld¹, Edwin Mientjes¹, Marianne van Tienhoven¹, Elodie Jadot⁵, Zhengxin Jiang⁶, Annemieke Verkerk⁷, Sigrid Swagemakers^{7,8}, Hanka Venselaar⁹, Zohreh Rahimi¹⁰, Hossein Najmabadi¹¹, Hanne Meijers-Heijboer¹², Esther de Graaff¹³, Wim A. Helbing⁴, Rob Willemsen¹, Koen Devriendt¹⁴, John W. Belmont⁶, Ben A. Oostra¹, Jeffrey D. Amack^{3,16}, and Aida M. Bertoli-Avella^{1,16,*}

¹Department of Clinical Genetics, Erasmus Medical Center, Rotterdam, The Netherlands
²Department of Cardiology, Erasmus Medical Center, Rotterdam, The Netherlands
³State University of New York Upstate Medical University, Department of Cell and Developmental Biology, Syracuse, New York, United States
⁴Department of Pediatric Cardiology, Erasmus Medical Center-Sophia, Rotterdam, The Netherlands
⁵Lille University of Sciences and Technologies, Lille, France
⁶Department of Molecular and Human Genetics, Baylor College of Medicine, Houston, United States
⁷Department of Bioinformatics, Erasmus Medical Center, Rotterdam, The Netherlands
⁸Department of Genetics, Erasmus Medical Center, Rotterdam, The Netherlands
⁹Center for Molecular and Biomolecular Informatics (CMBI) and Nijmegen Center for Molecular Life Sciences (NCMLS), Radboud University Nijmegen Medical Center, The Netherlands
¹⁰Medical Biology Research Center and Biochemistry Department, Medical School, Kermanshah University of Medical Sciences, Kermanshah, Iran
¹¹Genetics Research Center, University of Social Welfare and Rehabilitation Sciences, Tehran, Iran
¹²Department of Clinical Genetics, VU Medical Center, Amsterdam, The Netherlands
¹³Department of Cell Biology, Faculty of Science, Utrecht University, Utrecht, The Netherlands
¹⁴Department of Clinical Genetics, University Hospital Leuven, Leuven, Belgium

Abstract

Rationale—Congenital heart malformations are a major cause of morbidity and mortality especially in young children. Failure to establish normal left-right (L-R) asymmetry often results in cardiovascular malformations and other laterality defects of visceral organs.

Objective—To identify genetic mutations causing cardiac laterality defects.

Methods and Results—We performed a genome-wide linkage analysis in patients with cardiac laterality defects from a consanguineous family. The patients had combinations of defects that included dextrocardia, transposition of great arteries, double outlet right ventricle, atrio-ventricular septal defects and caval vein abnormalities. Sequencing of positional candidate genes identified mutations in *NPHP4*. We performed mutation analysis of *NPHP4* in 146 unrelated patients with

*Corresponding author: Dr. A.M. Bertoli-Avella, Dept. Clinical Genetics, Erasmus MC Rotterdam, P.O.Box 2040, 3000 CA, Rotterdam, The Netherlands. Tel: +31-10-7044628, Fax: +31-10-7044736, a.bertoliavella@erasmusmc.nl.

¹⁵These authors contributed equally

¹⁶These authors contributed equally

Disclosures

None.

similar cardiac laterality defects. Forty-one percent of these patients also had laterality defects of the abdominal organs. We identified eight additional missense variants that were absent or very rare in controls. To study the role of *nphp4* in establishing L-R asymmetry, we used antisense morpholinos to knockdown *nphp4* expression in zebrafish. Depletion of *nphp4* disrupted L-R patterning as well as cardiac and gut laterality. Cardiac laterality defects were partially rescued by human *NPHP4* mRNA, whereas mutant *NPHP4* containing genetic variants found in patients failed to rescue. We show that *nphp4* is involved in the formation of motile cilia in Kupffer's vesicle (KV), which generate asymmetric fluid flow necessary for normal L-R asymmetry.

Conclusions—*NPHP4* mutations are associated with cardiac laterality defects and heterotaxy. In zebrafish, *nphp4* is essential for the development and function of KV cilia and is required for global L-R patterning.

Keywords

Congenital heart malformations; heterotaxy; *nphp4*; cilia; zebrafish

Introduction

Laterality defects refer to a broad group of disorders caused by the disruption of normal left-right (L-R) asymmetry of the thoracic or abdominal visceral organs¹. *Situs inversus totalis* is the mirror image reversal of all visceral organs, whereas heterotaxy is the abnormal orientation of one or more organs along the L-R axis². In heterotaxy, congenital heart malformations result in major morbidity and mortality³. Although heterotaxy most often occurs as a sporadic condition, familial clustering has been documented with pedigrees suggesting autosomal recessive, autosomal dominant and X-linked inheritance⁴⁻⁷.

L-R patterning of vertebrate embryos occurs prior to organ formation and is conducted by a conserved signalling cascade that includes asymmetric expression of the *NODAL*, *LEFTY*, and *PITX2* genes in left lateral plate mesoderm (LPM)⁸. Motile cilia are involved in establishing this L-R asymmetric signaling. Laterality defects have been linked to ciliary motility by the observation that 48% of individuals with primary cilia dyskinesia also had *situs inversus totalis* and 6% had heterotaxy⁹.

Animal models have assisted our understanding of L-R patterning and the role of cilia. The *inversus viscerum* (*iv*) mouse has a mutation in the ciliary *left-right dynein* (*lrd*) gene and often develops laterality defects¹⁰. *Lrd* was found to be required for normal motility of monocilia on an embryonic structure called the node. These node cilia generate a leftward fluid flow that is necessary for normal asymmetric Nodal-Lefty-Pitx2 signaling¹¹. In zebrafish, Kupffer's vesicle is a ciliated organ analogous to the mouse node that is essential for normal L-R patterning¹². Asymmetric fluid flow generated by the monocilia may move signaling factors^{11, 13} and/or bend mechanosensory cilia¹⁴ to initiate asymmetric signaling.

Dysfunction of ciliary proteins gives rise to a wide range of human disorders known as ciliopathies. They can lead to a variety of defects including craniofacial, skeletal, respiratory, reproductive, renal, visual, olfactory and auditory abnormalities¹⁵⁻¹⁷. The nephronophthisis (NPHP) and associated ciliopathies - Senior-Loken syndrome, Joubert syndrome, Meckel-Gruber syndrome - are characterized by cilia-related defects, including cystic kidney disease, retinal degeneration, liver fibrosis and brain malformations¹⁸⁻¹⁹. Mutations in 18 genes are known to cause nephronophthisis and associated ciliopathies²⁰⁻²¹. Interestingly, mutations in *NPHP2/INVS* and *NPHP3* can also lead to heterotaxy, *situs inversus* and isolated congenital heart malformations²²⁻²⁴.

Protein network analysis has shown that several of these proteins form an interaction network organized in at least three connected modules: NPHP1-4-8, NPHP5-6 and MKS²⁵. Ciliary localization analysis of eight nephrocystins (NPHP1-6, 9 and 10) indicates that they are present in the primary cilia, the basal body and/or the centrioles and suggest that they participate in ciliary assembly and trafficking²⁵⁻²⁸.

In this study, a genome-wide linkage analysis identified *nephronophthisis-4* (*NPHP4*) variants in patients with cardiac laterality defects. Functional studies indicated that loss of zebrafish *nphp4* resulted in cardiac laterality defects. In addition, *nphp4* depletion disrupted asymmetric Nodal expression in the LPM, indicating *nphp4* is required for global L-R patterning of the embryo. Analysis of cilia in Kupffer's vesicle revealed that loss of *nphp4* reduced cilia length and disrupted asymmetric fluid flow. Our results establish the importance of *nphp4* in cilia development and function. Furthermore, our findings suggest that malfunction of *NPHP4* contributes to a wide range of congenital heart malformations and more complex defects within the heterotaxy spectrum.

Materials and Methods

An expanded Methods section is available in the Online Data Supplement.

Results

Clinical studies

We identified a consanguineous Iranian family including five patients with congenital heart malformations. Three patients (IV-1, IV-8 and IV-12; Figure 1a) were born with similar cardiac laterality defects (Table 1). Patient IV-1 had dextrocardia, atrial situs solitus, complete atrioventricular septal defect and discordant ventriculo-arterial connection with dextro-transposition of the great arteries (d-TGA). In addition, he had an interrupted inferior caval vein and a severe pulmonary valve stenosis (PS). He had no surgical correction and died suddenly at the age of 22 years. No autopsy was performed. Patient IV-8 had dextrocardia, dextrorotation and atrial situs solitus. She had an azygos continuation of the right infrahepatic part of the inferior caval vein draining into the right superior caval vein and the suprahepatic part of the inferior caval vein draining into the right atrium. She had a cor triatriatum with the right pulmonary veins draining into the right part of the left atrium and the left pulmonary veins into the left part of the left atrium. A persistent left inferior and superior caval vein also drained into the left part of the left atrium. She had a secundum atrial septal defect (ASD) and perimembranous ventricular septal defect (VSD). She had also left bronchial isomerism. Patient IV-12 had atrial situs solitus, atrio-ventricular concordance and ventriculo-arterial discordance namely, double outlet right ventricle and d-TGA. He also had a subpulmonary VSD, patent foramen ovale and patent ductus arteriosus (PDA).

In addition, patient IV-7 died shortly after birth due to an unspecified congenital heart malformation (Figure 1a). The fifth patient (IV-16) had mild congenital heart malformations consisting of a small VSD, PS and PDA, which was ligated at one year of age (Table 1).

Physical examination revealed no dysmorphisms and all patients had normal psychomotor development. CT/MRI or ultrasound of the abdomen revealed no kidney cysts and all individuals have reached adulthood at the time of their last evaluations. No abdominal laterality defects such as asplenia or polysplenia, malrotation of the gut or midline liver were detected in any of these cases. None of the patients had signs of abnormal mucociliary clearance. No visual problems or night blindness were reported.

Genome-wide linkage analysis

The genome-wide linkage analysis was performed using Affymetrix SNP arrays. Two unaffected parents, three patients and one healthy sibling (Figure 1a) were included in the analysis. Multipoint linkage analysis revealed five regions on chromosomes 1, 2, 3, 9 and 11 with LOD scores above 2.5 (Figure 1b). The maxLOD scores (2.7) were located on chromosome 1p36 and 11p15. Subsequently, microsatellite markers mapping to all candidate regions were tested. The loci on chromosomes 2, 3, and 9 were excluded, based on heterozygosity observed in the patients (data not shown).

On the chromosome 1p36 locus, all three patients with cardiac laterality defects (IV-1, IV-8 and IV-12) shared a homozygous region covered by 59 SNPs from rs4845835 to rs1203695. Haplotype analysis showed recombinations that delimited the borders of the region from rs2722782 (5.26 Mb) to rs1203696 (14.21 Mb) (Online Figure Ia). Thus, the candidate region spanned 9 Mb and contained 152 genes (NCBI build 37.1).

These patients also showed homozygous genotypes for 49 consecutive SNPs on chromosome 11, from rs16905816 to rs10500752. Further fine mapping in the 11p area delineated the borders of the linkage region between markers D11S4188 (telomeric) and rs2896598 (centromeric) (Online Figure Ib). The chromosome 11 locus extended only 3 Mb (9.1–12.1 Mb), containing 34 genes (NCBI build 37.1).

Haplotypes from both loci were examined in all available family members. A normal person (IV-14, with normal MRI of the thorax/abdomen) had homozygous haplotypes on the chromosome 1 locus (Online Figure Ia). In addition, individuals IV-3 and IV-4 were homozygotes for the chromosome 11 locus (Online Figure Ib); both persons were reported as unaffected, but medical examinations could not be performed. Patient IV-16, exhibiting a mild cardiac phenotype and no laterality defects, carried heterozygous haplotypes at both loci (data not shown). Only the three patients with laterality heart defects had homozygous haplotypes on both loci. Since these were the only genomic regions where the three patients showed extended homozygosity, we further investigated these loci.

Sequence analysis

A total of 109 genes on the chromosome 1p36 locus had a known reference sequence (NCBI build 37.1). Selection of genes for sequence analysis was based on available expression and/or functional information. The data was analyzed through the use of Ingenuity pathway analysis (Ingenuity® Systems). Thirty-six candidate genes were selected from the chromosome 1 locus. Direct sequencing of their coding regions identified two novel homozygous missense variants in the *NPHP4* gene present in three patients from the index family: c.3131G>A (p.Arg1044His) and c.3706G>A (p.Val1236Met) (Online Table I). These non-synonymous variants are extremely rare in the Iranian (Kurdish) population (allele frequency of 0.2% and 0.1% in 1232 control chromosomes). Moreover, the variants were absent in 270 Caucasian/Dutch and 178 Hispanic control chromosomes.

From the 34 genes mapping to the chromosome 11 locus, 19 genes had a well annotated reference sequence. Sequence analysis of their coding regions and exon-intron boundaries revealed only one novel DNA missense variant (Online Table I). In the *AMPD3* gene (*adenosine monophosphate deaminase 3*), the homozygous c.2240 G>A (p.Arg747Gln) variant was found. This variant was not present in 626 control chromosomes. Mutations in the *AMPD3* gene lead to (asymptomatic) deficiency of erythrocyte AMP deaminase²⁹ (OMIM 612874).

***NPHP4* variants in patients with laterality defects (heterotaxy)**

We sequenced all 30 exons of *NPHP4* in three cohorts of patients with cardiac laterality defects - with or without other situs abnormalities. Patient samples were collected at the Erasmus Medical Center, Rotterdam, the Department of Clinical Genetics, Leuven and from the Baylor College of Medicine, Houston. All 146 patients had a variety of cardiac laterality defects. Transposition of the great arteries was the most frequently found (49% of the patients). In addition, complete atrio-ventricular septal defect, double outlet right ventricle and abnormal pulmonary venous return were often reported. Dextrocardia was present in 33% of patients. Moreover, 41% had documented laterality defects of the abdominal organs, including abdominal *situs inversus*, asplenia or polysplenia, midline liver and intestinal malrotation.

Nine missense variants were found in 10 patients (Figure 1c, d and Table 1). The population frequency of each allele was tested by sequencing ethnically matched controls. A variant was considered as likely non-pathogenic if the allele frequency in healthy individuals was higher than 1%. Thus, p.Pro1160Leu with a frequency of 2.1% in control chromosomes was excluded from further analysis. In addition, we investigated the frequency of these variants in available databases (dbSNP135, 1000Genomes, NHLBI exome project). All variants were very rare or absent in controls (allele frequency 0.8%, Table 1).

These rare *NPHP4* variants were significantly more frequent in heterotaxy cases (6%, 9 of 146 cases) than in controls (1.2%, 3 of 250, Fisher's exact test $p=0.006$). *In silico* evaluation was performed using five prediction computer programs. This assessment predicted the impact of amino acid substitutions on the structure and function of human proteins. The variants were classified as probably pathogenic if at least 3 programs considered them as damaging (Table 1). Seven variants satisfied this criterion. Interestingly, p.Phe91Leu, p.Arg961His and p.Arg1192Trp have been reported in patients with Senior-Loken syndrome type 4 or nephronophthisis type 4³⁰.

Identification of zebrafish *nphp4* and characterization of its expression during embryogenesis

A zebrafish *nphp4* ortholog was taken from the Ensembl database (Online Figure II). To determine the pattern of *nphp4* expression during embryogenesis, we performed reverse transcription PCR (RT-PCR) and RNA *in situ* hybridization experiments at several developmental stages. Consistent with a recent report³¹ we found *nphp4* expression was maternally supplied and ubiquitously expressed during the first 24 hours of zebrafish development (Online Figure IIIb-g). RT-PCR detected *nphp4* expression at all stages tested between 4-cell stage and 100 hours post-fertilization (hpf) (Online Figure IIIa). This early and ubiquitous expression pattern suggested a role for *nphp4* during early development.

***nphp4* is required for normal cardiac laterality in zebrafish**

To assess the function of *nphp4* during embryonic development, we utilized antisense morpholino oligonucleotides (MO) to knockdown expression of zebrafish Nphp4 protein. Embryos injected with a MO designed to block *nphp4* mRNA translation (*nphp4* TB-MO) developed dose-dependent morphological abnormalities reminiscent of embryos with cilia defects³²⁻³⁴, including a curved body axis (Online Figure IVd) and otolith formation defects at 2 days post-fertilization (dpf) (Online Figure Va, b).

In addition, RNA *in situ* hybridization staining of the heart-specific marker *cmlc2* revealed heart laterality defects. Uninjected controls and embryos injected with a standard control MO showed normal rightward looping of the heart at 2 dpf (Figure 2a, b). However, heart

looping in *nphp4* TB-MO injected embryos was significantly altered, as the heart often looped in the reverse orientation or failed to loop (Figure 2a, b).

To test whether heart laterality phenotypes were specific to knockdown of *nphp4*, we designed two additional MOs to interfere with *nphp4* mRNA splicing at exon 4 (*nphp4* SB-MO1) or exon 9 (*nphp4* SB-MO2) (Online Figure IVa, b). Quantitative real time PCR (qPCR) analysis indicated *nphp4* SB-MO1 reduced *nphp4* mRNA levels by 90% (Online Figure IVc) and caused heart laterality defects without inducing body axis defects (Figure 2a, b and Online Figure IVd). This indicates heart L-R phenotypes are separable from axial defects. *nphp4* SB-MO2 reduced the amount of normally spliced *nphp4* mRNA by 50% (Online Figure IVc) and resulted in curved body axis and heart looping defects (Online Figure IVd and Figure 2a, b, respectively), similar to *nphp4* TB-MO injected embryos. Injecting a lower dose of *nphp4* SB-MO2 (0.4 ng) also altered heart looping, but with reduced penetrance (Figure 2b), suggesting partial loss of *nphp4* can cause cardiac laterality defects.

Other abnormalities such as hydrocephalus or gross eye defects were not observed. At 5 dpf, pronephric cysts were observed with a low penetrance in embryos injected with TB-MO (11%) or SB-MO2 (8%) (Online Figure Vc, d). No pronephric cysts were observed in SB-MO1 injected embryos. Our results using three independent MOs suggested a role for *nphp4* that is required for normal heart laterality in zebrafish.

To further confirm that defects observed in zebrafish embryos were specifically due to *nphp4* depletion, we conducted rescue experiments using human wild-type (wt) *NPHP4* mRNA. Co-injecting *nphp4* TB-MO with wt *NPHP4* mRNA resulted in a partial, but significant, rescue of heart looping defects (% of normal embryos improved from 43% to 60%, $p=0.03$; Figure 2c). Next, we co-injected *nphp4* TB-MO with human *NPHP4* mRNA containing either the c.3131G>A (p.Arg1044His) or c.3706G>A (p.Val1236Met) missense variant identified in the index family. In contrast to wt *NPHP4*, these *NPHP4* variants failed to rescue heart looping defects (Figure 2c). These results suggest that these variants are pathogenic and are involved in human laterality defects.

***nphp4* controls global L-R patterning of the zebrafish embryo**

To determine whether *nphp4* plays a role in heart laterality specifically or is involved in establishing global L-R patterning of the embryo, we analyzed additional markers of L-R asymmetry. RNA *in situ* hybridization, using *foxa3* probes to label the embryonic gut, showed that *nphp4* knockdown significantly altered laterality of the liver and pancreas in *nphp4* MO injected embryos (Figure 3a, b). We next analyzed expression of the Nodal-related gene *southpaw* (*spaw*), the earliest asymmetrically expressed gene in lateral plate mesoderm (LPM) in zebrafish³⁵. Control embryos exhibited normal left-sided *spaw* expression (Figure 3c, d). In contrast, *nphp4* MO injected embryos showed a significant disruption of *spaw* expression, which was often reversed, bilateral or absent (Figure 3c, d). Altered asymmetric gene expression can result from defects in the embryonic midline³⁶. However, analysis of the midline markers *no tail* and *sonic hedgehog* revealed that midline structures were intact in *nphp4* MO injected embryos (Online Figure VI). These results indicate *nphp4* functions independent of midline development to control *spaw* expression and global L-R patterning of the embryo.

***nphp4* is required for normal cilia length and directional fluid flow in Kupffer's vesicle**

In zebrafish, Kupffer's vesicle (KV) is a transient organ that generates cilia-driven asymmetric fluid flow necessary to bias *spaw* expression to the left LPM. Examination of live embryos at the 8 somite stage showed that the KV organ appeared normal in control

MO (Figure 4a) and *nphp4* MO injected embryos (Figure 4b, c). However, analysis of cilia in KV by fluorescent immunostaining with acetylated Tubulin antibodies revealed that the cilia were significantly shorter in *nphp4* MO injected embryos (Figure 4e-g) as compared to controls (Figure 4d, g). We did not observe a significant difference of KV cilia number between control and *nphp4* MO injected embryos (Figure 4h). To analyze KV cilia function, we injected fluorescent beads into KV of live embryos and used video microscopy to record fluid flow¹². Most control embryos showed strong counter-clockwise asymmetric fluid flow (Figure 4i, l; Movie S1). In contrast, flow was often absent (Figure 4j, l; Movie S2) or reduced (Figure 4k, l; Movie S3) in *nphp4* MO injected embryos. Consistent with dose-dependent effects of *nphp4* SB-MO2 on heart looping (Figure 2b), we observed more severe flow defects in embryos injected with a higher *nphp4* SB-MO2 dose (Figure 4l). Together, these results show that *nphp4* knockdown results in short KV cilia and compromises asymmetric fluid flow that is necessary for normal L-R patterning.

Discussion

We found homozygous missense *NPHP4* variants in a consanguineous family containing three patients with cardiac laterality defects, bronchial isomerism and normal abdominal situs. Interestingly, though *NPHP4* is a cilia related gene that is mutated in patients with autosomal recessive juvenile nephronophthisis (NPHP type 4, OMIM 606966)³⁷ and Senior-Loken syndrome (SLSN4, OMIM 606996)³⁸, our patients did not show signs of nephronophthisis or retinitis pigmentosa, which are distinctive features of these diseases.

Because of the known interaction between *NPHP1*, *NPHP2/INVS*, *NPHP3* and *NPHP4* proteins^{23-24, 37}, it is obvious that mutations in one or more of these genes disrupt the same pathway(s) and can lead to similar phenotypes (i.e. nephronophthisis). Conversely, mutations within the same gene can lead to various phenotypic outcomes in different patients. Mutations in *NPHP2* result in nephronophthisis with or without *situs inversus* and mild cardiac defects²³ whereas *NPHP3* mutations lead to isolated nephronophthisis or retinal degeneration³⁹. Alternately, *NPHP3* mutations can cause a broad clinical spectrum of early embryonic patterning defects comprising of *situs inversus*, congenital heart defects, central nervous system malformations and renal-hepatic-pancreatic dysplasia²⁴. The *NPHP6* gene (*CEP290*) is another good example. The phenotypic spectrum of the mutations ranges from isolated blindness, SLSN, nephronophthisis, Joubert syndrome, Bardet-Biedl syndrome, to the lethal Meckel-Grüber syndrome⁴⁰.

We investigated the presence of *NPHP4* variants in 146 sporadic patients having cardiac laterality defects, with or without involvement of other thoracic or abdominal organs. In 6% of the patients, we identified heterozygous missense variants compared to 1.2% of the ethnically matched controls, indicating mutation excess in the patients ($p < 0.006$). No compound heterozygous or homozygous variants were detected in these sporadic cases. Similarly, single heterozygous *NPHP4* variants were found in the majority of patients with autosomal recessive nephronophthisis type 4³⁰. A second mutation might be located in an area not covered by exon sequencing or in another (cilia-related) gene. The latest, a complex genetic model with combined effects of multiple genes seems the most plausible explanation. In fact, di- or oligogenic inheritance have been demonstrated in several ciliopathies, including the nephronophthisis^{21, 41}, Joubert syndrome⁴² and Bardet Biedl syndrome⁴³⁻⁴⁴.

The findings in our study are entirely consistent with a complex, oligogenic disease model. The rare heterozygous variants identified in the sporadic cases have probably an epistatic effect with additional genetic modifiers. Even in the index consanguineous family, we

cannot exclude the existence of other genetic variants that explain the complex cardiovascular malformations and heterotaxy and the lack of renal/visual disease.

In congenital heart malformations and heterotaxy, the NODAL signaling pathway is a paradigm for oligogenic inheritance. Some patients with heterotaxy and/or conotruncal defects such as double outlet right ventricle (DORV) and transposition of great arteries (TGA), show several mutations in genes belonging to the NODAL signaling pathway^{45–46}. As functional significance of mutations in these genes were demonstrated, the cumulative effects of multiple mutations may lead to reduced NODAL signaling eventually resulting in congenital heart malformations. In addition, a combinatorial role between the NODAL signaling pathway and *ZIC3* gene has been demonstrated in familial TGA patients⁴⁷. These studies support the notion that genetic variants or susceptibility alleles within one or more developmental pathways may dysregulate signaling in a synergistic fashion and cause congenital heart malformations or heterotaxy.

Studies in humans, zebrafish and mice indicate that *NPHP2* and *NPHP3* play a role in L-R axis determination^{22–24, 39}. To investigate the role of *NPHP4* in establishing L-R asymmetry, we used antisense MOs to knockdown expression of zebrafish *nphp4*. Depletion of *nphp4* in zebrafish resulted in abnormal heart and gut orientation, closely resembling the (cardiac) laterality defects observed in the patients. Co-injection of *nphp4* TB-MO and human wt *NPHP4* mRNA significantly ameliorated the phenotypic spectrum due to *nphp4* depletion. In contrast, co-injection of *nphp4* TB-MO and human *NPHP4* mRNA containing genetic variants found in patients failed to rescue the laterality defects suggesting that these variants are pathogenic. Furthermore, analysis of asymmetric gene expression revealed that *nphp4* knockdown alters asymmetric Nodal expression in the LPM without affecting expression of midline markers.

Our analyses in zebrafish have confirmed that knockdown of *nphp4* results in shortened motile cilia⁴⁸. For first time we show that *nphp4* depletion leads to disruption of cilia-driven fluid flow within KV which most likely cause laterality defects. Similarly, *nphp3* knockdown in zebrafish leads to *situs inversus* and heterotaxy due to defective (fewer and shorter) KV cilia⁴⁹.

In conclusion, we identified *NPHP4* mutations in patients with cardiac laterality defects and other malformations within the heterotaxy spectrum. In zebrafish, our results demonstrate that *nphp4* is required for global L-R patterning of the embryo via regulation of Nodal signaling and plays a role that is essential for the development and function of KV cilia.

The linking of *NPHP4* to L-R axis determination and laterality defects will help dissect the complex genetic composition of heterotaxy and related cardiovascular malformations.

Supplementary Material

Refer to Web version on PubMed Central for supplementary material.

Acknowledgments

We are grateful to the family and patients and who participated in the study.

We thank Fiona Foley, Chunlei Gao and Herma van der Linde for excellent technical assistance and Tom de Vries Lentsch for the artwork. We acknowledge Prof. Peter van der Spek for the use of Ingenuity Systems.

Sources of funding

This work was partially funded by the Dutch Heart Foundation, the Netherlands (2006T006) to I.M.B.H. L., an Erasmus MC grant and an Erasmus Fellowship (Erasmus Medical Center, The Netherlands) to A.M. B-A, a grant from the Center for Biomedical Genetics (CBG), the Netherlands to B.A.O., and a grant from the National Heart Lung and Blood Institute, USA, (R01HL095690) to J.D.A.

Non-standard Abbreviations and Acronyms

| | |
|-------------------|--|
| L-R | Left-right |
| LPM | Lateral plate mesoderm |
| NPHP | Nephronophthisis |
| SLSN | Senior-Loken syndrome |
| KV | Kupffer's vesicle |
| LOD scores | Logarithm of the Odds |
| MO | Morpholino oligonucleotides |
| TB-MO | Translation blocking MO |
| SB-MO | Splicing blocking MO |
| ASD | Atrial septal defect |
| VSD | Ventricular septal defect |
| AVSD | Atrioventricular septal defect |
| MV | Mitral valve |
| TGA | Transposition of great arteries (Dextro or Levo) |
| DORV | Double outlet right ventricle |
| PDA | Persistent ductus arteriosus |
| BAV | Bicuspid aortic valve |
| AS | Aortic stenosis |
| PA | Pulmonary atresia |
| PV | Pulmonary valve |
| PS | Pulmonary valve stenosis |
| HLHS | Hypoplastic left heart syndrome |
| CoA | Coarctation of the aorta |
| TAPVR | Total anomalous pulmonary venous return |
| ICV | Inferior caval vein |
| SCV | Superior caval vein |
| Het | Heterozygous |
| Hom | Homozygous |

References

1. Bisgrove BW, Morelli SH, Yost HJ. Genetics of human laterality disorders: Insights from vertebrate model systems. *Annu Rev Genomics Hum Genet.* 2003; 4:1–32. [PubMed: 12730129]
2. Jacobs JP, Anderson RH, Weinberg PM, Walters HL 3rd, Tchervenkov CI, Del Duca D, Franklin RC, Aiello VD, Beland MJ, Colan SD, Gaynor JW, Krogmann ON, Kurosawa H, Maruszewski B,

- Stellin G, Elliott MJ. The nomenclature, definition and classification of cardiac structures in the setting of heterotaxy. *Cardiol Young*. 2007; 17(Suppl 2):1–28. [PubMed: 18039396]
3. Sutherland MJ, Ware SM. Disorders of left-right asymmetry: Heterotaxy and situs inversus. *Am J Med Genet C Semin Med Genet*. 2009; 151C:307–317. [PubMed: 19876930]
 4. Belmont JW, Mohapatra B, Towbin JA, Ware SM. Molecular genetics of heterotaxy syndromes. *Curr Opin Cardiol*. 2004; 19:216–220. [PubMed: 15096953]
 5. Gebbia M, Ferrero GB, Pilia G, Bassi MT, Aylsworth A, Penman-Splitt M, Bird LM, Bamforth JS, Burn J, Schlessinger D, Nelson DL, Casey B. X-linked situs abnormalities result from mutations in *zic3*. *Nat Genet*. 1997; 17:305–308. [PubMed: 9354794]
 6. Vitale E, Brancolini V, De Rienzo A, Bird L, Allada V, Sklansky M, Chae CU, Ferrero GB, Weber J, Devoto M, Casey B. Suggestive linkage of situs inversus and other left-right axis anomalies to chromosome 6p. *J Med Genet*. 2001; 38:182–185. [PubMed: 11303511]
 7. Wessels MW, De Graaf BM, Cohen-Overbeek TE, Spitaels SE, de Groot-de Laat LE, Ten Cate FJ, Frohn-Mulder IF, de Krijger R, Bartelings MM, Essed N, Wladimiroff JW, Niermeijer MF, Heutink P, Oostra BA, Dooijes D, Bertoli-Avella AM, Willems PJ. A new syndrome with noncompaction cardiomyopathy, bradycardia, pulmonary stenosis, atrial septal defect and heterotaxy with suggestive linkage to chromosome 6p. *Hum Genet*. 2008; 122:595–603. [PubMed: 17938964]
 8. Zhu L, Belmont JW, Ware SM. Genetics of human heterotaxias. *Eur J Hum Genet*. 2006; 14:17–25. [PubMed: 16251896]
 9. Kennedy MP, Omran H, Leigh MW, Dell S, Morgan L, Molina PL, Robinson BV, Minnix SL, Olbrich H, Severin T, Ahrens P, Lange L, Morillas HN, Noone PG, Zariwala MA, Knowles MR. Congenital heart disease and other heterotaxic defects in a large cohort of patients with primary ciliary dyskinesia. *Circulation*. 2007; 115:2814–2821. [PubMed: 17515466]
 10. Supp DM, Witte DP, Potter SS, Brueckner M. Mutation of an axonemal dynein affects left-right asymmetry in *inversus viscerum* mice. *Nature*. 1997; 389:963–966. [PubMed: 9353118]
 11. Nonaka S, Tanaka Y, Okada Y, Takeda S, Harada A, Kanai Y, Kido M, Hirokawa N. Randomization of left-right asymmetry due to loss of nodal cilia generating leftward flow of extraembryonic fluid in mice lacking *kif3b* motor protein. *Cell*. 1998; 95:829–837. [PubMed: 9865700]
 12. Essner JJ, Amack JD, Nyholm MK, Harris EB, Yost HJ. Kupffer's vesicle is a ciliated organ of asymmetry in the zebrafish embryo that initiates left-right development of the brain, heart and gut. *Development*. 2005; 132:1247–1260. [PubMed: 15716348]
 13. Tanaka Y, Okada Y, Hirokawa N. Fgf-induced vesicular release of sonic hedgehog and retinoic acid in leftward nodal flow is critical for left-right determination. *Nature*. 2005; 435:172–177. [PubMed: 15889083]
 14. McGrath J, Somlo S, Makova S, Tian X, Brueckner M. Two populations of node monocilia initiate left-right asymmetry in the mouse. *Cell*. 2003; 114:61–73. [PubMed: 12859898]
 15. Baker K, Beales PL. Making sense of cilia in disease: The human ciliopathies. *Am J Med Genet C Semin Med Genet*. 2009; 151C:281–295. [PubMed: 19876933]
 16. Bisgrove BW, Yost HJ. The roles of cilia in developmental disorders and disease. *Development*. 2006; 133:4131–4143. [PubMed: 17021045]
 17. Fliegauf M, Benzing T, Omran H. When cilia go bad: Cilia defects and ciliopathies. *Nat Rev Mol Cell Biol*. 2007; 8:880–893. [PubMed: 17955020]
 18. Hildebrandt F, Attanasio M, Otto E. Nephronophthisis: Disease mechanisms of a ciliopathy. *J Am Soc Nephrol*. 2009; 20:23–35. [PubMed: 19118152]
 19. Hildebrandt F, Zhou W. Nephronophthisis-associated ciliopathies. *J Am Soc Nephrol*. 2007; 18:1855–1871. [PubMed: 17513324]
 20. Hurd TW, Hildebrandt F. Mechanisms of nephronophthisis and related ciliopathies. *Nephron Exp Nephrol*. 2011; 118:e9–e14. [PubMed: 21071979]
 21. Otto EA, Ramaswami G, Janssen S, Chaki M, Allen SJ, Zhou W, Airik R, Hurd TW, Ghosh AK, Wolf MT, Hoppe B, Neuhaus TJ, Bockenhauer D, Milford DV, Soliman NA, Antignac C, Saunier S, Johnson CA, Hildebrandt F. Mutation analysis of 18 nephronophthisis associated ciliopathy disease genes using a DNA pooling and next generation sequencing strategy. *J Med Genet*. 2010; 10:10.

22. Chaki M, Hoefele J, Allen SJ, Ramaswami G, Janssen S, Bergmann C, Heckenlively JR, Otto EA, Hildebrandt F. Genotype-phenotype correlation in 440 patients with nphp-related ciliopathies. *Kidney Int.* 2011; 80:1239–1245. [PubMed: 21866095]
23. Otto EA, Schermer B, Obara T, O'Toole JF, Hiller KS, Mueller AM, Ruf RG, Hoefele J, Beekmann F, Landau D, Foreman JW, Goodship JA, Strachan T, Kispert A, Wolf MT, Gagnadoux MF, Nivet H, Antignac C, Walz G, Drummond IA, Benzing T, Hildebrandt F. Mutations in *invs* encoding inversin cause nephronophthisis type 2, linking renal cystic disease to the function of primary cilia and left-right axis determination. *Nat Genet.* 2003; 34:413–420. [PubMed: 12872123]
24. Bergmann C, Fliegauf M, Bruchle NO, Frank V, Olbrich H, Kirschner J, Schermer B, Schmedding I, Kispert A, Kranzlin B, Nurnberg G, Becker C, Grimm T, Girschick G, Lynch SA, Kelehan P, Senderek J, Neuhaus TJ, Stallmach T, Zentgraf H, Nurnberg P, Gretz N, Lo C, Lienkamp S, Schafer T, Walz G, Benzing T, Zerres K, Omran H. Loss of nephrocystin-3 function can cause embryonic lethality, meckel-gruber-like syndrome, situs inversus, and renal-hepatic-pancreatic dysplasia. *Am J Hum Genet.* 2008; 82:959–970. [PubMed: 18371931]
25. Sang L, Miller JJ, Corbit KC, Giles RH, Brauer MJ, Otto EA, Baye LM, Wen X, Scales SJ, Kwong M, Huntzicker EG, Sfakianos MK, Sandoval W, Bazan JF, Kulkarni P, Garcia-Gonzalo FR, Seol AD, O'Toole JF, Held S, Reutter HM, Lane WS, Rafiq MA, Noor A, Ansar M, Devi AR, Sheffield VC, Slusarski DC, Vincent JB, Doherty DA, Hildebrandt F, Reiter JF, Jackson PK. Mapping the nphp-jbts-mks protein network reveals ciliopathy disease genes and pathways. *Cell.* 2011; 145:513–528. [PubMed: 21565611]
26. Shiba D, Manning DK, Koga H, Beier DR, Yokoyama T. *Inv* acts as a molecular anchor for nphp3 and nek8 in the proximal segment of primary cilia. *Cytoskeleton (Hoboken).* 67:112–119. [PubMed: 20169535]
27. Shiba D, Yokoyama T. The ciliary transitional zone and nephrocystins. *Differentiation.* 2011; 12:12.
28. Shiba D, Yamaoka Y, Hagiwara H, Takamatsu T, Hamada H, Yokoyama T. Localization of *inv* in a distinctive intraciliary compartment requires the c-terminal ninein-homolog-containing region. *J Cell Sci.* 2009; 122:44–54. [PubMed: 19050042]
29. Yamada Y, Goto H, Ogasawara N. A point mutation responsible for human erythrocyte AMP deaminase deficiency. *Hum Mol Genet.* 1994; 3:331–334. [PubMed: 8004104]
30. Hoefele J, Sudbrak R, Reinhardt R, Lehrack S, Hennig S, Imm A, Muerb U, Utsch B, Attanasio M, O'Toole JF, Otto E, Hildebrandt F. Mutational analysis of the nphp4 gene in 250 patients with nephronophthisis. *Hum Mutat.* 2005; 25:411. [PubMed: 15776426]
31. Slanchev K, Putz M, Schmitt A, Kramer-Zucker A, Walz G. Nephrocystin-4 is required for pronephric duct-dependent cloaca formation in zebrafish. *Hum Mol Genet.* 2011; 20:3119–3128. [PubMed: 21596840]
32. Kramer-Zucker AG, Olale F, Haycraft CJ, Yoder BK, Schier AF, Drummond IA. Cilia-driven fluid flow in the zebrafish pronephros, brain and Kupffer's vesicle is required for normal organogenesis. *Development.* 2005; 132:1907–1921. [PubMed: 15790966]
33. Colantonio JR, Vermot J, Wu D, Langenbacher AD, Fraser S, Chen JN, Hill KL. The dynein regulatory complex is required for ciliary motility and otolith biogenesis in the inner ear. *Nature.* 2009; 457:205–209. [PubMed: 19043402]
34. Gao C, Wang G, Amack JD, Mitchell DR. *Oda16/wdr69* is essential for axonemal dynein assembly and ciliary motility during zebrafish embryogenesis. *Dev Dyn.* 2010; 239:2190–2197. [PubMed: 20568242]
35. Long S, Ahmad N, Rebagliati M. The zebrafish nodal-related gene *southpaw* is required for visceral and diencephalic left-right asymmetry. *Development.* 2003; 130:2303–2316. [PubMed: 12702646]
36. Tabin CJ. The key to left-right asymmetry. *Cell.* 2006; 127:27–32. [PubMed: 17018270]
37. Mollet G, Salomon R, Gribouval O, Silbermann F, Bacq D, Landthaler G, Milford D, Nayir A, Rizzoni G, Antignac C, Saunier S. The gene mutated in juvenile nephronophthisis type 4 encodes a novel protein that interacts with nephrocystin. *Nat Genet.* 2002; 32:300–305. [PubMed: 12244321]

38. Otto E, Hoefele J, Ruf R, Mueller AM, Hiller KS, Wolf MT, Schuermann MJ, Becker A, Birkenhager R, Sudbrak R, Hennies HC, Nurnberg P, Hildebrandt F. A gene mutated in nephronophthisis and retinitis pigmentosa encodes a novel protein, nephroretinin, conserved in evolution. *Am J Hum Genet.* 2002; 71:1161–1167. [PubMed: 12205563]
39. Olbrich H, Fliegauf M, Hoefele J, Kispert A, Otto E, Volz A, Wolf MT, Sasmaz G, Trauer U, Reinhardt R, Sudbrak R, Antignac C, Gretz N, Walz G, Schermer B, Benzing T, Hildebrandt F, Omran H. Mutations in a novel gene, *nphp3*, cause adolescent nephronophthisis, tapeto-retinal degeneration and hepatic fibrosis. *Nat Genet.* 2003; 34:455–459. [PubMed: 12872122]
40. Coppieters F, Lefever S, Leroy BP, De Baere E. *Cep290*, a gene with many faces: Mutation overview and presentation of *cep290base*. *Hum Mutat.* 2010; 31:1097–1108. [PubMed: 20690115]
41. Hoefele J, Wolf MT, O'Toole JF, Otto EA, Schultheiss U, Deschenes G, Attanasio M, Utsch B, Antignac C, Hildebrandt F. Evidence of oligogenic inheritance in nephronophthisis. *J Am Soc Nephrol.* 2007; 18:2789–2795. [PubMed: 17855640]
42. Tory K, Lacoste T, Burglen L, Moriniere V, Boddaert N, Macher MA, Llanas B, Nivet H, Bensman A, Niaudet P, Antignac C, Salomon R, Saunier S. High *nphp1* and *nphp6* mutation rate in patients with joubert syndrome and nephronophthisis: Potential epistatic effect of *nphp6* and *ahl1* mutations in patients with *nphp1* mutations. *J Am Soc Nephrol.* 2007; 18:1566–1575. [PubMed: 17409309]
43. Katsanis N, Ansley SJ, Badano JL, Eichers ER, Lewis RA, Hoskins BE, Scambler PJ, Davidson WS, Beales PL, Lupski JR. Triallelic inheritance in bardet-biedl syndrome, a mendelian recessive disorder. *Science.* 2001; 293:2256–2259. [PubMed: 11567139]
44. Katsanis N, Eichers ER, Ansley SJ, Lewis RA, Kayserili H, Hoskins BE, Scambler PJ, Beales PL, Lupski JR. *Bbs4* is a minor contributor to bardet-biedl syndrome and may also participate in triallelic inheritance. *Am J Hum Genet.* 2002; 71:22–29. [PubMed: 12016587]
45. Roessler E, Ouspenskaia MV, Karkera JD, Velez JI, Kantipong A, Lacbawan F, Bowers P, Belmont JW, Towbin JA, Goldmuntz E, Feldman B, Muenke M. Reduced nodal signaling strength via mutation of several pathway members including *foxf1* is linked to human heart defects and holoprosencephaly. *Am J Hum Genet.* 2008; 83:18–29. [PubMed: 18538293]
46. Mohapatra B, Casey B, Li H, Ho-Dawson T, Smith L, Fernbach SD, Molinari L, Niesh SR, Jefferies JL, Craigen WJ, Towbin JA, Belmont JW, Ware SM. Identification and functional characterization of nodal rare variants in heterotaxy and isolated cardiovascular malformations. *Hum Mol Genet.* 2009; 18:861–871. [PubMed: 19064609]
47. De Luca A, Sarkozy A, Consoli F, Ferese R, Guida V, Dentici ML, Mingarelli R, Bellacchio E, Tuo G, Limongelli G, Digilio MC, Marino B, Dallapiccola B. Familial transposition of the great arteries caused by multiple mutations in laterality genes. *Heart.* 2010; 96:673–677. [PubMed: 19933292]
48. Burckle C, Gaude HM, Vesque C, Silbermann F, Salomon R, Jeanpierre C, Antignac C, Saunier S, Schneider-Maunoury S. Control of the wnt pathways by nephrocystin-4 is required for morphogenesis of the zebrafish pronephros. *Hum Mol Genet.* 2011; 20:2611–2627. [PubMed: 21498478]
49. Zhou W, Dai J, Attanasio M, Hildebrandt F. Nephrocystin-3 is required for ciliary function in zebrafish embryos. *Am J Physiol Renal Physiol.* 2010; 299:F55–F62. [PubMed: 20462968]

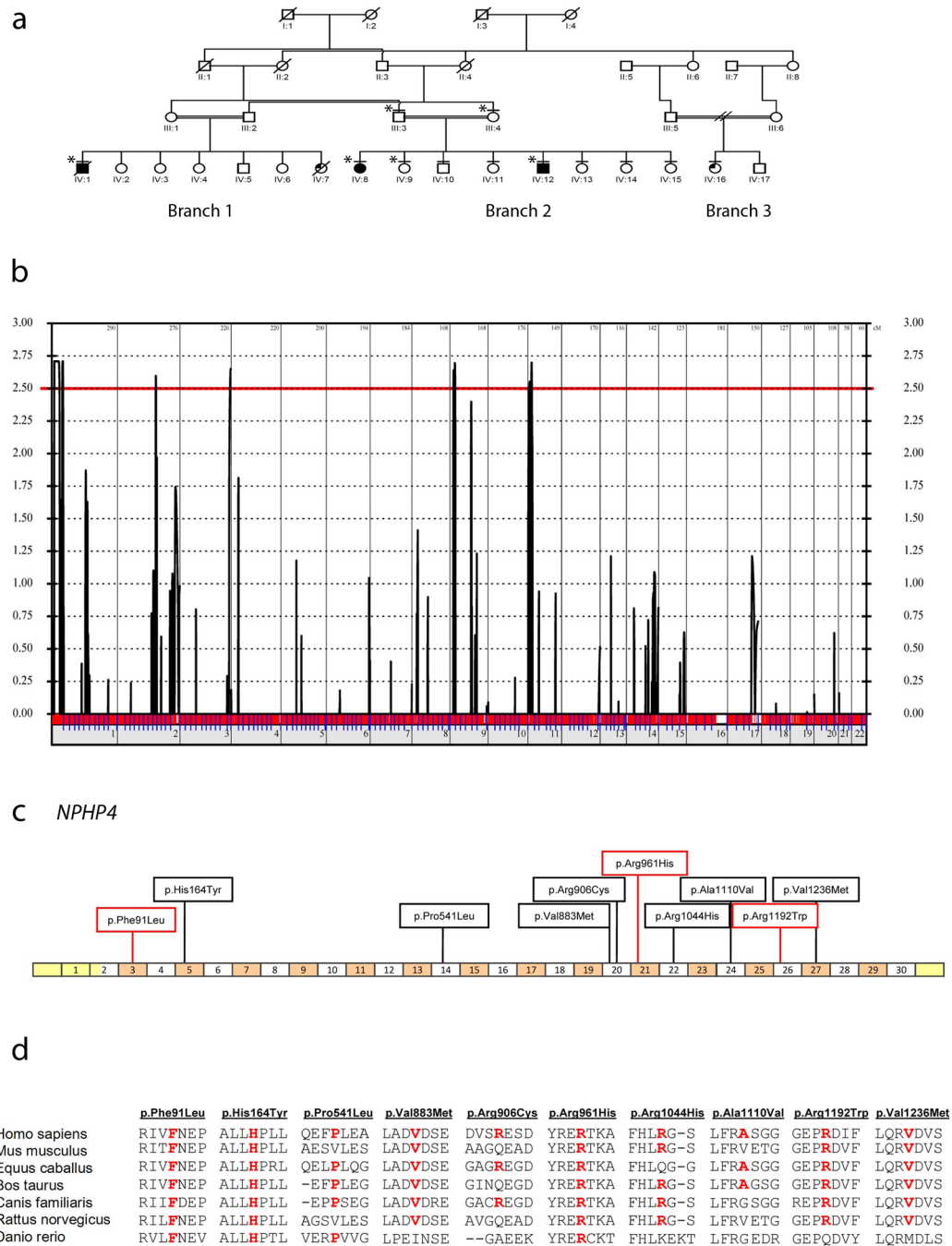


Figure 1. Genome-wide Linkage Analysis (GWLA) and *NPHP4* variants identification
(a) Simplified genealogical tree of the index family. A horizontal line above the symbol indicates medical examination. Open symbols indicate normal individuals, solid black symbols indicate patients with cardiac laterality defects and quarter-filled symbols indicate presence of other congenital heart malformations. The double line between individuals indicates consanguinity and the diagonal line through a symbol is a deceased family member. Individuals labeled with an asterisk (*) were included in the GWLA. For the genetic analysis, all individuals in whom medical examination was not possible were considered as “phenotype unknown.” **(b)** Multipoint LOD scores: X-axis represents all

human autosomes and Y-axis corresponds to the LOD scores. Chromosomal regions with LOD scores above 2.5 (red horizontal line) were further investigated. **(c)** Summary of the *NPHP4* variations identified in patients of the index family, the Dutch and the American cohorts. White and peach colored boxes represent exons and yellow boxes represent untranslated regions. Red-boxed variants were previously described in SLSN4 or NPHP4 patients. **(d)** Alignment of NPHP4 protein with several species. The illustrated protein segments were derived from Ensembl reference sequences. Red letters indicate amino acid residues identical to those of human.

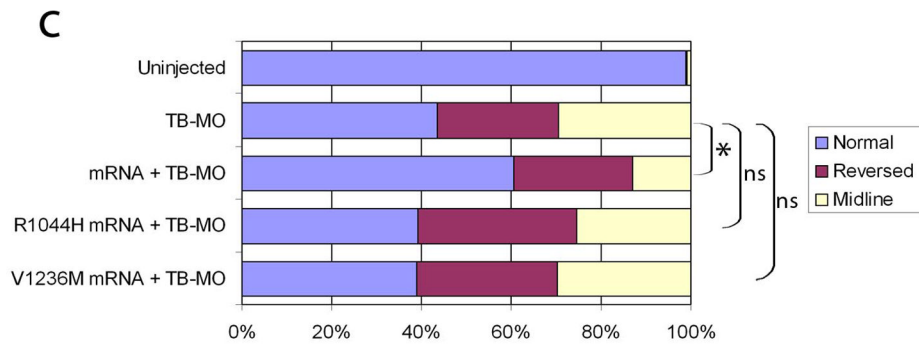
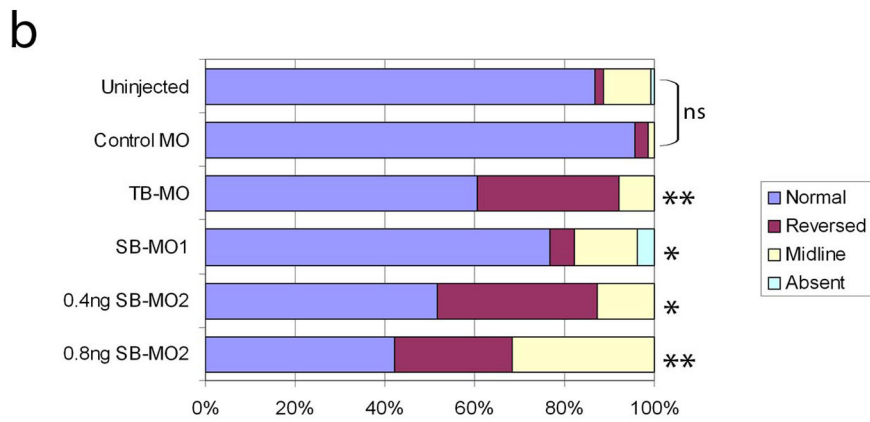
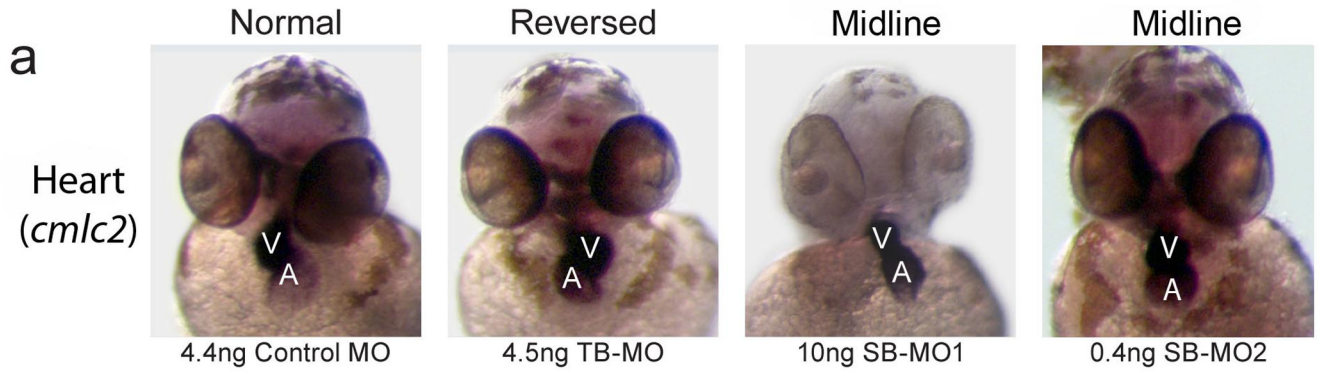


Figure 2. *nphp4* knockdown alters zebrafish heart laterality. Wild-type, but not mutant, human *NPHP4* mRNA partially rescues zebrafish *nphp4* phenotype

(a) *in situ* hybridizations using a heart-specific probe (*cmlc2*) showed that embryos injected with a control MO had predominantly normal cardiac looping. In contrast, heart laterality was often reversed or remained along the midline in *nphp4* MO injected embryos.

V=ventricle, A=atrium, (b) The distributions of heart orientation observed in uninjected embryos (n=242), Control MO (n=71), *nphp4* TB-MO (n=89), *nphp4* SB-MO1 (n=106) and *nphp4* SB-MO2 (0.8ng, n=76 and 0.4ng n=95) embryos. (c) Human wt *NPHP4* mRNA partially rescued heart laterality defects; the graph shows the distribution of normal and abnormal heart looping in uninjected embryos (n=239), embryos injected with 4.5ng TB-

MO (n=154) and injected with both 100pg human wt *NPHP4* mRNA and 4.5ng TB-MO (n=249). In contrast, mutant *NPHP4* containing either the p.Arg1044His (n=189) or p.Val1236Met (n=188) missense variants failed to rescue the phenotype (4.5ng TB-MO and 100pg mutant *NPHP4* mRNA). * p 0.038; ** p 2.6×10^{-4} , ns: not significant.

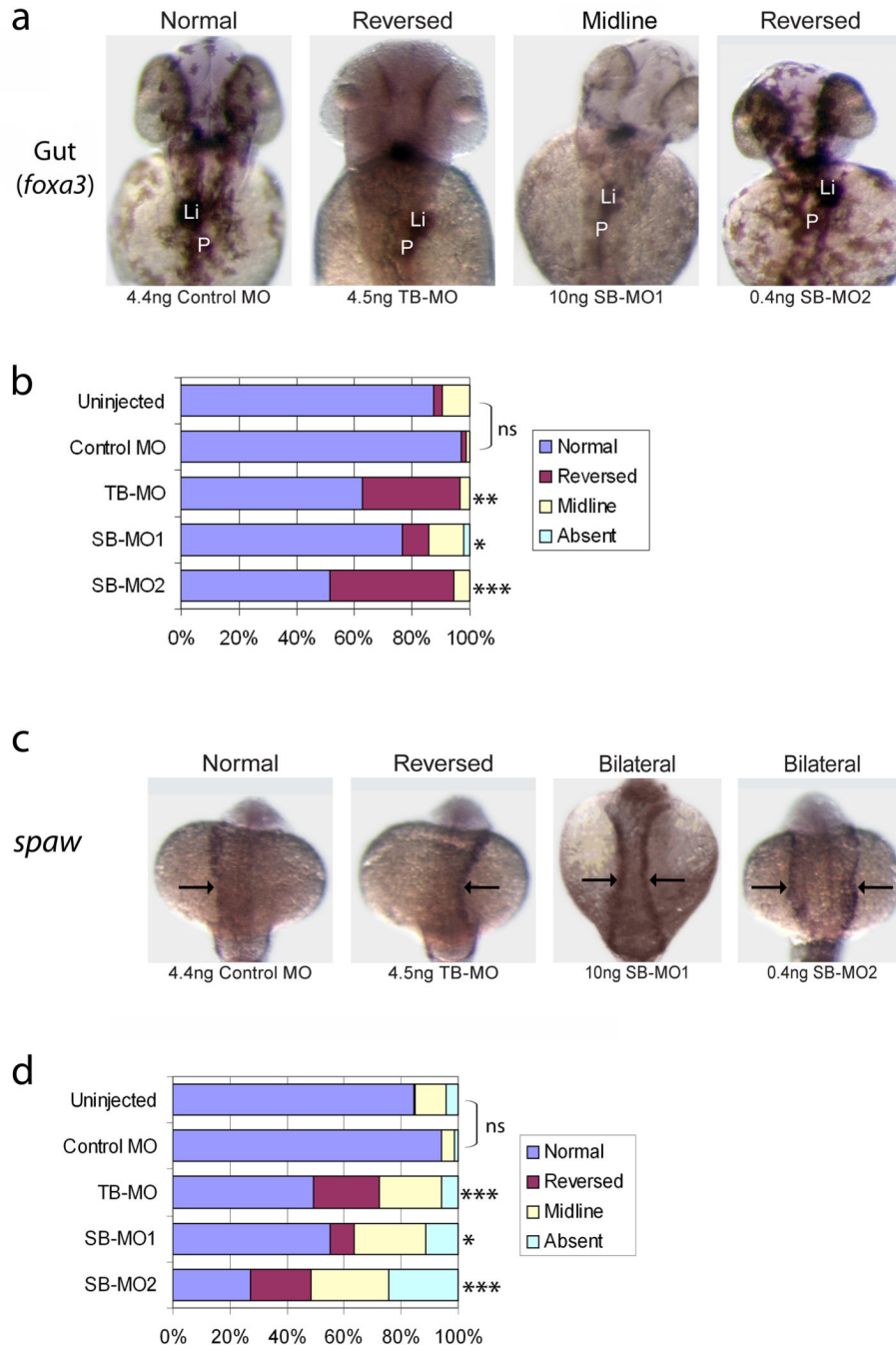


Figure 3. *nphp4* knockdown alters zebrafish gut laterality and disrupts global asymmetric gene expression

(a) *in situ* hybridizations using a gut-specific probe (*foxa3*) showed that embryos injected with a control MO had predominantly normal liver and pancreas orientation. In contrast, gut laterality was often reversed or remained along the midline in *nphp4* MO injected embryos. Li=liver, P=pancreas (b) The distributions of gut orientation observed in uninjected embryos (n=242), Control MO (n=71), *nphp4* TB-MO (n=89), *nphp4* SB-MO1 (n=106) and *nphp4* SB-MO2 (n=76) injected embryos. (c) *in situ* hybridization staining of *southpaw* (*spaw*) expression (arrows) in lateral plate mesoderm at 16–18 SS. *spaw* expression, which is normally left-sided in controls was often reversed, bilateral or absent in *nphp4* MO injected

embryos. **(d)** The distributions of *spaw* expression patterns in uninjected embryos (n=217), Control MO (n=88), *nphp4* TB-MO (n=134), *nphp4* SB-MO1 (n=116) and *nphp4* SB-MO2 (n=70) embryos. **p* 0.028; ***p* 0.0012 and ****p* 5.9×10^{-4} , ns: not significant.

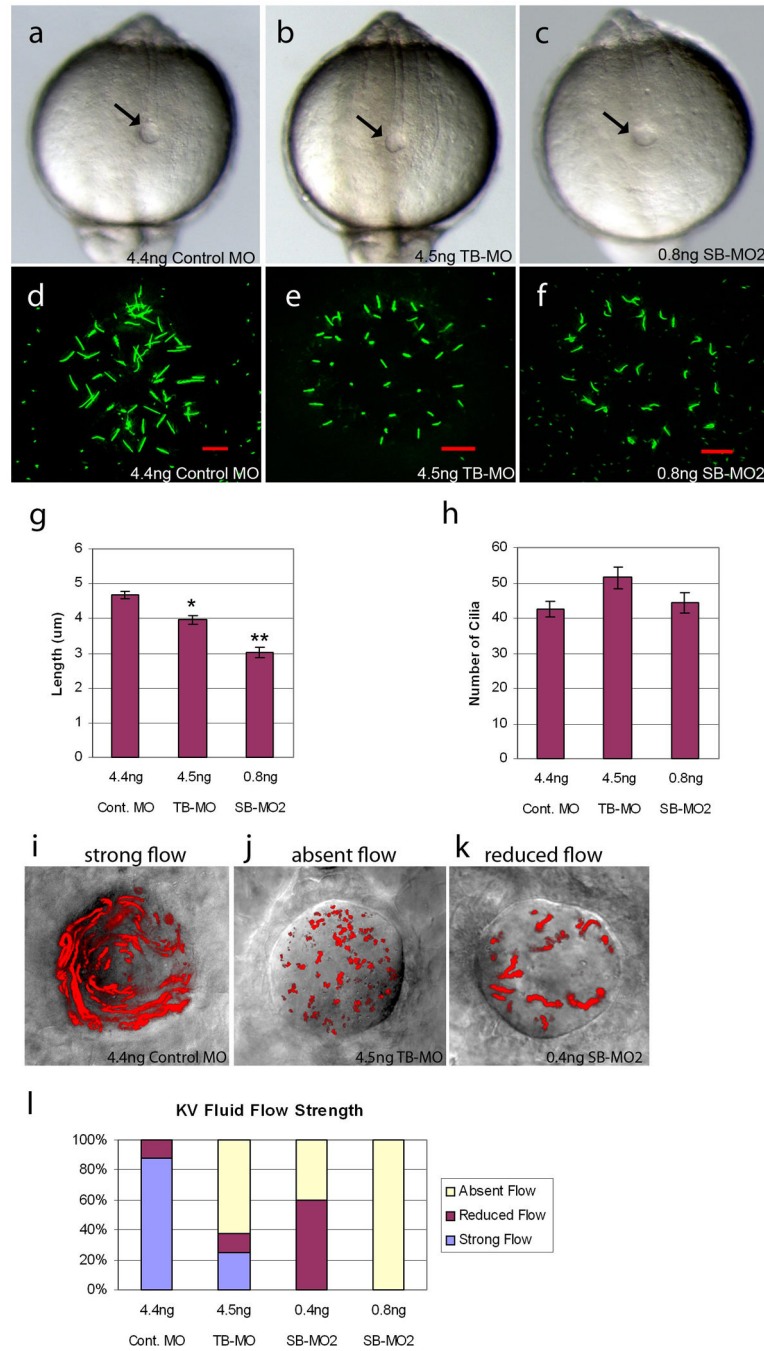


Figure 4. *nphp4* knockdown shortens cilia and disrupts fluid flow in Kupffer's vesicle (KV) (a-c) KV (arrow) appeared similar in live control MO (a), *nphp4* TB-MO (b) and *nphp4* SB-MO2 (c) embryos at 8 SS. (d-f) Visualization of KV cilia using anti-acetylated tubulin antibodies at 8 SS revealed shorter cilia in *nphp4* MO embryos (e,f), relative to controls (d). Red scale bar represents 10 µM. (g-h) Graphs show the average KV cilia length (g) and number (h) in control MO (n=38), *nphp4* TB-MO (n=21) and *nphp4* SB-MO2 (n=25) embryos at 8 SS. Error bars represent standard error of the mean. * $p < 0.0001$ and ** $p < 3 \times 10^{-12}$ when compared to control MO embryos (Student's t-test). (i-k) Fluorescent bead paths (red) superimposed on images of KV of representative embryos at 8 to 10 SS.

Strong directional flow (i) was observed in most control MO injected embryos (i), whereas flow was often absent (j) or reduced (k) in *nphp4* TB-MO and *nphp4* SB-MO2 embryos. **(l)** The percentage of embryos classified with a strong, reduced or absent fluid flow. Embryos were injected with control MO (n=17), *nphp4* TB-MO (n=8), 0.4 ng (lower dose) *nphp4* SB-MO2 (n=5) or 0.8 ng *nphp4* SB-MO2 (n=4).

TABLE 1

NPHP4 variants found in patients with cardiovascular malformations with or without laterality defects of other thoracic or abdominal organs. All variants are absent or rare (<1%) in control populations.

| Patient details | | | | Clinical features | | | | <i>NPHP4</i> genotypes | | | |
|-----------------|-------------------|---------|-----|--|---|---|------------------------|------------------------------|----------------------|-------------------------|--|
| Family | Origin | Patient | Sex | Cardiovascular abnormalities | Other organs asymmetry | Other features | Coding variant | Protein effect | Doses | Prediction ¹ | Freq. in controls ² |
| 1 | Iranian | IV-1 | M | Dextrocardia, D-TGA, ASD, VSD, AVSD, PS, interrupted ICV | - | - | c.3131G>A c.3706G>A | p.Arg1044His p.Val1236Met | Hom 5, 6 Hom 5, 6 | Pathogenic Neutral | 0.2% (2/1232) 0.01% (1/6887) 0.1% (1/1232) 0% |
| 1 | Iranian | IV-8 | F | Dextrocardia, ASD, VSD, interrupted ICV with azygous continuation, persistent left SCV and ICV, con trinitium | Left lung isomerism | - | c.3131G>A c.3706G>A | p.Arg1044His p.Val1236Met | Hom 5, 6 Hom 5, 6 | Pathogenic Neutral | 0.2% (2/1232) 0.01% (1/6887) 0.1% (1/1232) 0% |
| 1 | Iranian | IV-12 | M | D-TGA, DORV, VSD, PDA | - | - | c.3131G>A c.3706G>A | p.Arg1044His p.Val1236Met | Hom 5, 6 Hom 5, 6 | Pathogenic Neutral | 0.2% (2/1232) 0.01% (1/6887) 0.1% (1/1232) 0% |
| 1 | Iranian | IV-16 | F | VSD, PS, PDA | - | - | c.3131G>A c.3706G>A | p.Arg1044His p.Val1236Met | Het Het | Pathogenic Neutral | 0.2% (2/1232) 0.01% (1/6887) 0.1% (1/1232) 0% |
| 2 | Dutch, Chinese | 02D3049 | F | VSD, PA | Right lung isomerism, abdominal situs inversus | Large splenic cyst | c.3329C>T | p. Ala1110Val | Het | Neutral | 0.6% (2/318) 0.01% (1/6887) rs139767853 |
| 3 | Dutch, Cape Verde | 07D2466 | F | Dextrocardia, AVSD, PS, L-TGA, DORV | Right lung isomerism, midline liver, asplenia | - | c.1622C>T | p. Pro541Leu | Het | Pathogenic | 0% (0/182) 0.3% (30/9810) rs145255635 |
| 4 | Caucasian | LAT0025 | M | Mesocardia | Abdominal situs inversus, Midline liver and intestinal malrotation | Cholelithiasis, omphalocele, small spleen | c.271T>C | p. Phe91Leu ³ | Het | Pathogenic | 0% (0/180) 0.1% (10/6766) |
| 5 | Caucasian | LAT0033 | F | Mesocardia, atrial inversion, VSD, ASD, PA, D-TGA, DORV, severe aortic root dilation | Abdominal situs inversus, Midline liver | - | c.490C>T | p. His164Tyr | Het 5 | Pathogenic | 0% (0/180) 0% |
| 6 | Caucasian | LAT1268 | M | HLHS, VSD, ASD, MV hypoplasia, BAV, CoA, PDA, interrupted ICV with azygous continuation | Polysplenia, transverse liver, midline gall bladder and portal vein, intestinal malrotation | Right hydronephrosis | c.2647G>A | p. Val883Met | Het 6 | Neutral | 0% (0/122) 0.01% (1/6887) |
| 7 | Caucasian | LAT0079 | M | Common atrium, right atrial isomerism, single ventricle, AVSD, PA, azygous continuation to right SCV | Abdominal situs inversus | - | c.2716C>T | p. Arg90Cys | Het | Pathogenic | 0% (0/122) 0% |
| 8 | Caucasian | LAT1168 | M | Right atrial isomerism, single ventricle, ASD, MV atresia, PS, DORV, VSD, infra-diaphragmatic TAPVR, absent ICV with azygous continuation to ipsilateral SCV, persistent left SCV to coronary sinus, right aortic arch with a common broncho-splenic trunk, abnormal branching pattern of the abdominal vessels from the aorta | Abdominal situs inversus, asplenia and intestinal malrotation | - | c.2882G>A | p. Arg96His ⁴ | Het 5 | Pathogenic | 0.5% (1/182) 0.4% (30/6952) |
| 9 | Hispanic | LAT0145 | M | HLHS, AVSD, D-TGA, DORV, bicuspid PV, PS, supracardiac TAPVR | Midline liver, asplenia and intestinal malrotation | Mild hepatomegaly with calcifications, cholelithiasis, Hypothyroidism | c.3574C>T | p. Arg1192Trp ⁴ | Het 6 | Pathogenic | 0% (0/182) 0.3% (21/6625) rs139022622 |

| Patient details | | | | Clinical features | | | NPHP4 genotypes | | | | |
|-----------------|-----------|---------|-----|--|------------------------|----------------|-----------------|----------------|-------|-------------------------|---|
| Family | Origin | Patient | Sex | Cardiovascular abnormalities | Other organs asymmetry | Other features | Coding variant | Protein effect | Doses | Prediction ¹ | Freq. in controls ² |
| 10 | Caucasian | LAT1034 | M | Single ventricle, MV atresia, VSD, ASD, subvalvular AS, PS, L-TGA, DORV, PDA | - | - | c.3329C>T | p. Ala110Val | Het | Neutral | 0.6% (2,318) 0.8% (56/6872) 15139/67853 |

Abbreviations: ASD Atrial septal defect, VSD Ventricular septal defect, AVSD: Atrioventricular septal defect, MV: Mitral valve, TGA Transposition of great arteries (Dextro or Levo), DORV Double outlet right ventricle, PDA Persistent ductus arteriosus, BAY Bicuspid aortic valve, AS Aortic stenosis, PA Pulmonary atresia, PV Pulmonary valve, PS Pulmonary valve stenosis, HLHS Hypoplastic left heart syndrome, CoA Coarctation of the aorta, TAPVR Total anomalous pulmonary venous return, ICV Inferior caval vein, SCV Superior caval vein.

Het: Heterozygous, Hom: Homozygous

¹ Prediction of the genetic variant effect on protein level (Pmut, SNPs3D, SIFT, PolyPhen, HOPE)

² Based on ethnically matched (in house) control chromosomes and the frequencies reported by the NHLBI Exome Sequencing Project

³ Reported in patients with SLSN4

⁴ Reported in patients with NPHP4

⁵ Inherited from father

⁶ Inherited from mother

⁷ Total allele counts include European and African American population.